

Semi-metric portfolio optimization: a new algorithm reducing simultaneous asset shocks

Nick James^a (nick.james@unimelb.edu.au), Max Menzies^b
(menzies@tsinghua.edu.cn), Jennifer Chan^c (jennifer.chan@sydney.edu.au)

^a School of Mathematics and Statistics, University of Melbourne, Victoria 3010,
Australia

^b Yau Mathematical Sciences Center, Tsinghua University, Beijing 100084, China

^c School of Mathematics and Statistics, University of Sydney, NSW 2006, Australia

Corresponding Author:

Nick James

School of Mathematics and Statistics, University of Melbourne, Victoria 3010,
Australia

Tel: +61 433 952 207

Email: nick.james@unimelb.edu.au

Semi-metric portfolio optimization: a new algorithm reducing simultaneous asset shocks

Nick James^{a,*}, Max Menzies^{b,*}, Jennifer Chan^c

^a*School of Mathematics and Statistics, University of Melbourne, Victoria 3010, Australia*

^b*Yau Mathematical Sciences Center, Tsinghua University, Beijing 100084, China*

^c*School of Mathematics and Statistics, University of Sydney, NSW 2006, Australia*

Abstract

This paper proposes a new method for financial portfolio optimization based on reducing simultaneous asset shocks across a collection of assets. We apply recently introduced semi-metrics between finite sets to determine the distance between time series' structural breaks. Then, we build on the classical portfolio optimization theory of Markowitz and use this distance between asset structural breaks for our penalty function, rather than portfolio variance. Our experiments are promising: on synthetic data, we show that our proposed method does indeed diversify among time series with highly similar structural breaks, and enjoys advantages over existing metrics between sets. On real data, experiments illustrate that our proposed optimization method produces higher risk-adjusted returns than mean-variance portfolio optimization. Moreover, the predictive distribution is superior in every measure analyzed, producing a higher mean, lower standard deviation and lower kurtosis. The main implication for this method in portfolio management is reducing simultaneous asset shocks and potentially sharp associated drawdowns during periods of highly similar structural breaks, such as a market crisis.

Keywords: Portfolio optimization, Time series analysis, Change point detection, Similarity measures, Market crises

^{*}Equal contribution.

Email addresses: nick.james@unimelb.edu.au (Nick James), menzies@tsinghua.edu.cn (Max Menzies), jennifer.chan@sydney.edu.au (Jennifer Chan)

1. Introduction

Modern portfolio theory provides a framework for determining an allocation of weights in an investment portfolio by optimizing a specific objective function. The idea was first introduced by Markowitz (1952), and has progressed considerably since then. Markowitz' fundamental contribution was the concept of diversification among stock portfolios, rather than analyzing risk and return on an individual security basis. One of the most notable advancements was the work of Sharpe (1966), who proposed a measure of risk-adjusted returns in financial portfolios, the Sharpe ratio. This ratio is an indication of the potential reward in any candidate investment relative to its risk. The standard mathematical representation of the Sharpe ratio is the following optimization problem: given a collection of n assets, let R_i be the historical returns for the i th asset in a collection, Σ be the matrix of historical covariances between stocks, R_f the risk-free rate, and w_i the weights of the portfolio. One maximizes the Sharpe ratio:

$$\frac{\mathbb{E}(R_p) - R_f}{\sigma_p^2}, \text{ where} \quad (1)$$

$$\mathbb{E}(R_p) = \sum_{i=1}^n w_i R_i, \text{ and} \quad (2)$$

$$\sigma_p^2 = \mathbf{w}^T \Sigma \mathbf{w}. \quad (3)$$

This objective function selects an allocation of weights based on a trade-off between portfolio returns and variance. Returns are estimated from historical returns as $\mathbb{E}(R_p) = \sum_{i=1}^n w_i R_i$, while variance is $\sigma_p^2 = \mathbf{w}^T \Sigma \mathbf{w}$ where $\Sigma_{i,j}$ is the covariance between historical returns of assets i, j .

One may also impose certain conditions, depending on the context, which manifest as constraints, to accompany the objective function. Two typical constraint, which we impose throughout the paper, are $0 \leq w_i \leq 1, i = 1, \dots, n$ and $\sum_{i=1}^n w_i = 1$. These conditions require all portfolio assets to be invested and prohibit short-selling, respectively. Weights are chosen by maximizing the objective function subject to such conditions.

There has been significant research within the applied mathematics and computer science communities building upon Markowitz' mean-variance model (Markowitz, 1952; Sharpe, 1966). A variety of portfolio optimization frameworks have explored alternative objective functions utilizing risk measures other than standard volatility (Almahdi & Yang, 2017; Calvo et al., 2014; Soleimani et al., 2009; Vercher et al., 2007). Many authors in the field have taken existing theory and methodologies for the problem of portfolio selection and optimization (Bhansali, 2007; Moody & Saffell, 2001; Magdon-Ismail et al.), including clustering (Iorio et al., 2018; León et al., 2017) fuzzy sets (Tanaka et al., 2000; Kocadağlı & Keskin, 2015), regularization (Fastrich et al., 2014; Li, 2015; Pun & Wong, 2019) regression trees (Cappelli et al., 2021) and multi-objective optimization (Mansour et al., 2019).

1.1. Overview of change point detection methods

Many domains in the physical and social sciences are interested in the identification of structural breaks in various data sets. Ranshous et al. (2015) and Akoglu et al. (2014) recently provided an overview of anomaly detection methods within the context of network analysis, which can be used to identify relations among entities in high dimensional data. Koutra et al. (2016) determined change points (structural breaks) in dynamic networks via graph-based similarity measures, while James et al. (2021) analyzed change points in cryptocurrencies.

In the more statistical literature, focused on time series data, researchers have developed change point models driven by hypothesis tests, where p -values allow scientists to quantify the confidence in their algorithm (Moreno & Neville, 2013; Bridges et al., 2015; Peel & Clauset, 2015). Change point algorithms generally fall within statistical inference (namely, Bayesian) or hypothesis testing frameworks. Bayesian change point algorithms (Barry & Hartigan, 1993; Xuan & Murphy, 2007; Adams & MacKay, 2007) identify change point in a probabilistic manner and allow for subjectivity through the use of prior distributions, but suffer from hyperparameter sensitivity and do not provide statistical error bounds (p -values), often leading to a lack of reliability.

Within hypothesis testing, Ross (2015) outlined algorithmic developments in various change point models initially proposed by Hawkins (1977). Some of the more important developments in recent years include the work of Hawkins et al. (2003), and Ross et al. (Ross & Adams, 2012; Ross et al., 2013; Ross, 2014). Ross (2015) recently created the CPM package, which allows for flexible implementation of various change point models on time series data. Given the package's ease of use and flexibility, we build our methodology on this suite of algorithms.

1.2. Overview of semi-metrics

The application of metric spaces has provided the groundwork for research advancement in various areas of machine learning. In addition to more traditional metrics, such as the *Hausdorff* and *Wasserstein*, *semi-metrics*, which may not satisfy the triangle inequality property of a metric, have been used successfully in various machine learning applications. An overview of such (semi-)metrics and applications was recently provided by Conci & Kubrusly (2017). The three primary applications include image analysis (Baddeley, 1992; Dubuisson & Jain, 1994; Gardner et al., 2014), distance between fuzzy sets (Brass, 2002; Fujita, 2013; Gardner et al., 2014; Rosenfeld, 1985) and computational methods (Eiter & Mannila, 1997; Atallah, 1983; Atallah et al., 1991; Shonkwiler, 1989). More recently, a review and computational analysis of various (semi)-metrics was undertaken by James et al. (2020) in measuring distance between time series' sets of structural breaks.

2. Proposed semi-metric change point optimization framework

Our main contribution is to adapt the classical penalty function involving variance with one related to structural breaks. In many circumstances, variance is a suitable measure in a financial securities context. However, it is not without its limitations, and there are several reasons why a penalty function related to structural breaks may be a suitable alternative or complement to the covariance measure between two time series:

1. Covariance is computed as an expectation $\text{Cov}(X, Y) = \mathbb{E}(X - \mathbb{E} X)(Y - \mathbb{E} Y)$, which is an average (integral) over an entire probability space. In a financial context, this computes an average over time; in modern financial markets, especially since the global financial crisis, most time periods are bull markets, with most assets performing quite well together. As such, assets that rise together in a bull market but actually exhibit distinct dynamics may be erroneously identified as similar.
2. Covariance fails to capture dissimilarity between time series during periods of market crisis and erratic behavior. Investors are often particularly concerned with the robustness of their portfolio during such times. Portfolios that are optimized using covariance as a risk measure fail to determine the impact of various asset combinations during times of market crisis. For instance, if two assets are simultaneously acting erratically, they may actually be negatively correlated during this time. If they are both included in a portfolio, this would increase rather than reduce erratic behavior. Structural breaks herald erratic behavior, so using distances between breaks in the objective function may better separate out erratic behavior in a portfolio.
3. Investors are also interested in peak-to-trough measures of asset performance, that is, the size of a drop in returns from a local maximum to a local minimum. Optimization algorithms using covariance measures fail to identify and minimize peak-to-trough behavior. However, distances between sets of structural breaks (in the mean, variance and other stochastic quantities) are better equipped to identify how similar two time series are with respect to peak-to-trough measures. Thus, they may suitably allocate weights to minimize these precipitous drops.

We formulate our new objective function to penalize structural breaks and their associated erratic behavior. We use the MJ_p family of semi-metrics of James et al. (2020). Given $p > 0$ and two non-empty finite sets $S, T \subset \mathbb{R}$ (or an

arbitrary metric space), this is defined as

$$d_{MJ}^p(S, T) = \left(\frac{\sum_{t \in T} d(t, S)^p}{2|T|} + \frac{\sum_{s \in S} d(s, T)^p}{2|S|} \right)^{\frac{1}{p}}. \quad (4)$$

where $d(s, T)$ is the minimal distance from a point $s \in S$ to the finite set T . We note $d(S, T) = 0$ if and only if $S = T$. As discussed by James et al. (2020), varying $p > 0$ produces a family of semi-metrics, where larger values of p exhibit greater adherence to the triangle inequality property, but worse sensitivity to outliers. In our implementation, we select $p = 0.5$ due to its good performance with outlier sensitivity, and the strong possibility of outliers in this context. Indeed, it is likely that some assets are impacted by market dynamics to which others are immune, which will yield outlier assets.

We compute a distance matrix D_{ij} as follows: following a suitable change point algorithm (ours is described in Appendix A), let asset i have set of structural breaks $S_i, i = 1, \dots, n$. Then we form

$$D_{ij} = d_{MJ}^{0.5}(S_i, S_j). \quad (5)$$

In this paper, every set of structural breaks, simulated or real, is non-empty, so this computation is possible. Next, we transform our distance matrix into an affinity matrix, which mimics the properties of a covariance matrix:

$$A_{ij} = 1 - \frac{D_{ij}}{\max D}, \forall i, j. \quad (6)$$

Two assets have correlation equal to 1 if and only if they are perfectly correlated; analogously, $A_{ij} = 1$ if and only if $d(S_i, S_j) = 0$, meaning the two assets have identical structural breaks.

In the context of Markowitz portfolio optimization, weights are chosen to maximize return while reducing total variance: this introduces more stocks with lower correlation, increases diversification and reduces systematic risk in the portfolio. We modify this insight, allocating weights that maximize return while

reducing affinity between sets of structural breaks and hence maximizing the spread between erratic behavior. To do so, we substitute our adjusted affinity matrix A for the original covariance matrix Σ , and optimize a new risk-adjusted return measure with respect to portfolio weights. We term this the MJ ratio objective function:

$$\frac{\mathbb{E}(R_p) - R_f}{\Omega_p}, \text{ where} \quad (7)$$

$$\mathbb{E}(R_p) = \sum_{i=1}^n w_i R_i, \text{ and} \quad (8)$$

$$\Omega_p = \mathbf{w}^T A \mathbf{w}. \quad (9)$$

We retain the same constraints as Section 1, $0 \leq w_i \leq 1, i = 1, \dots, n$ and $\sum_{i=1}^n w_i = 1$, for the remainder of our experiments section, but our method is flexible enough to vary such constraints. For example, the condition that every asset must be invested could be relaxed by treating cash as its own possible asset to hold.

3. Theoretical properties

In this section, we examine the mathematical properties of our proposed objective function, and explain our choice of distance function between sets, including an analysis of alternatives.

Proposition 3.1. *The MJ ratio, as presented in (7), can be maximized on the chosen domain of weights, and the maximum can be determined analytically.*

Proof. First we note that the matrix A is not necessarily positive-semi-definite, so standard arguments regarding the optimization of the Sharpe ratio do not apply *mutatis mutandis* to the MJ ratio. Instead, we require a continuity and compactness argument. Due to the conditions on the weights, the ratio is optimized over a space $S = \{w_i : 0 \leq w_i \leq 1, \sum_{i=1}^n w_i = 1\}$. This is a compact space, specifically a $(n-1)$ -simplex. By the definition of (6), all entries of A are non-negative, with diagonal elements equal to 1. Thus, $w^T A w$ is a continuous

function on S that attains only positive values and so the denominator of (7) is positive on the whole space S . This implies the MJ ratio is a well-defined continuous function on S . Since S is compact, it must achieve a global maximum on S .

Finally, since S is a $(n - 1)$ -simplex, one can examine and test the critical points within the simplex and use Lagrange multipliers on the boundary to find all possible maxima and test them. In our implementation, we determine the optimal weights with a simple grid search. \square

In the following two propositions, we justify our selection of distance measure between finite sets, specifically two advantages it has over the popular Hausdorff and Wasserstein metrics between sets.

Definition 3.2 (Hausdorff metric). Let S, T be closed bounded subsets of \mathbb{R} (or an arbitrary metric space). Their Hausdorff distance is defined by

$$d_H(S, T) = \max \left(\sup_{s \in S} d(s, T), \sup_{t \in T} d(t, S) \right), \quad (10)$$

$$= \sup \{d(s, T), s \in S; d(t, S), t \in T\}, \quad (11)$$

where $d(s, T) = \inf_{t \in T} d(s, t)$ is the infimum distance from s to T .

One could conceivably use this metric to measure distance between structural breaks, rather than our semi-metric. However, the Hausdorff metric suffers from substantial sensitivity to outliers, as observed by Baddeley (1992). We formalize this in the following proposition:

Proposition 3.3. *Let $T = \{t_1, \dots, t_n\}$ and S be fixed. Fixing all but one element, if $t_n \rightarrow \infty$ acts as an outlier, then the asymptotic behavior of the Hausdorff and $MJ_{0.5}$ distances are as follows:*

$$d_H(S, T) \sim |t_n|, \quad d_{MJ}^p(S, T) \sim \frac{|t_n|}{(2|T|)^{\frac{1}{p}}}, \quad (12)$$

$$\text{i.e. } \lim_{|t_n| \rightarrow \infty} \frac{d_H(S, T)}{|t_n|} = 1, \lim_{|t_n| \rightarrow \infty} \frac{d_{MJ}^p(S, T)}{|t_n|} = \frac{1}{(2|T|)^{\frac{1}{p}}}. \quad (13)$$

Proof. For both $d_H(S, T)$ and $d_{MJ}^p(S, T)$, the only term that increases as $|t_n| \rightarrow \infty$ is $d(t_n, S)$, which increases asymptotically with $|t_n|$. The result follows immediately for d_H and follows for d_{MJ}^p by inspecting the coefficient $\frac{1}{2|T|}$ that accompanies the term $d(t_n, S)$. \square

As a consequence of this outlier sensitivity property, the Hausdorff metric d_H may excessively grant an excessively high distance, and hence a low affinity, based on a single outlier structural breaks. In particular, two time series that have quite similar structural breaks (and hence erratic behavior profiles) may be granted low affinity and both included in a portfolio based on just one structural break. On the other hand, the MJ_p semi-metric handles outliers well, increasingly well with small values p , such as our choice in implementation $p = 0.5$. We illustrate an example of this in Section 4.1.

The other metric occasionally used to measure distance between finite sets is the Wasserstein metric. To be precise, it is most frequently employed between probability measures on a metric space, such as \mathbb{R} , as follows: let μ, ν be probability measures on \mathbb{R} , and $q \geq 1$, then

$$W_q(\mu, \nu) = \inf_{\gamma} \left(\int_{\mathbb{R} \times \mathbb{R}} |x - y|^q d\gamma \right)^{\frac{1}{q}}. \quad (14)$$

This infimum is taken over all joint probability measures γ on $\mathbb{R} \times \mathbb{R}$ with marginal probability measures μ and ν . The formula (14) is difficult to compute in general, but in the case where μ, ν have cumulative distribution functions F, G on \mathbb{R} , there is a simple representation (del Barrio et al., 1999):

$$W_q(\mu, \nu) = \left(\int_0^1 |F^{-1} - G^{-1}|^q dx \right)^{\frac{1}{q}}, \quad (15)$$

where F^{-1} is the inverse cumulative distribution function, or more precisely, quantile function, associated to F (Gilchrist, 2000). One can then use this to define a metric between finite sets S, T . One associates to each set a probability

measure defined as a weighted sum of Dirac delta measures

$$\mu_S = \frac{1}{|S|} \sum_{s \in S} \delta_s. \quad (16)$$

Then, the Wasserstein metric between sets S, T can be defined as $d_W^q(S, T) := W_q(\mu_S, \mu_T)$ and computed with (15). One could conceivably use this metric to measure distance between structural breaks instead of the Hausdorff metric. However, the Wasserstein metric has a property that makes it unsuitable in our context. Using the definition (16) and the equation (15), the Wasserstein metric has a geometric property with respect to translation, $d_W^q(S, S + a) = |a|$. However, this is unsuitable for measuring the distance between sets with high intersection. We formalize these remarks in the following proposition:

Proposition 3.4. *If $|S \cap T| = r$, the following inequality holds:*

$$d_{MJ}^p(S, T) \leq \left[1 - \frac{r}{2} \left(\frac{1}{|S|} + \frac{1}{|T|} \right) \right]^{\frac{1}{p}} d_H(S, T). \quad (17)$$

No such inequality holds for Wasserstein metric. Given a set S and its translation $S + a$ for some $a \in \mathbb{R}$, the Wasserstein metric has the property that $d_W^q(S, S + a) = |a|$. As a consequence, even with $|S \cap T| = |S| - 1 = |T| - 1$, it is possible for $d_W^q(S, T)$ to coincide with $d_H(S, T)$.

Proof. Examining the definition (4), any $d(s, T)$ or $d(t, S)$ term with $s \in S \cap T$ or $t \in S \cap T$, respectively, vanishes. Any other $d(s, T), d(t, S)$ term is at most $d_H(S, T)$. So

$$d_{MJ}^p(S, T) \leq \left[\frac{1}{2|S|} (|S| - r) + \frac{1}{2|T|} (|T| - r) \right] d_H(S, T), \quad (18)$$

which gives the inequality after simplifying. Turning to the Wasserstein metric, let $S = \{s_1, \dots, s_n\} \subset \mathbb{R}$ be a set with $s_1 < s_2 < \dots < s_n$ and $a \in \mathbb{R}$ a translate. Then $S + a = \{s_1 + a, \dots, s_n + a\}$. By (15) and (16), $d_W^q(S, S + a)$ can be

computed as

$$\left(\int_0^1 |F^{-1} - G^{-1}|^q dx \right)^{\frac{1}{q}}, \quad (19)$$

where F^{-1}, G^{-1} are the quantile functions associated to μ_S and μ_{S+a} . By integrating μ_S and μ_{S+a} , we can see that F, G are piecewise constant increasing step functions:

$$F = \sum_{j=1}^{n-1} \frac{j}{n} \mathbb{1}_{[s_j, s_{j+1})} + \mathbb{1}_{[s_n, \infty)}, \quad G = \sum_{j=1}^{n-1} \frac{j}{n} \mathbb{1}_{[s_j+a, s_{j+1}+a)} + \mathbb{1}_{[s_n+a, \infty)}. \quad (20)$$

It follows that their respective quantile functions are determined almost everywhere as

$$F^{-1} = \sum_{j=1}^n s_j \mathbb{1}_{(\frac{j-1}{n}, \frac{j}{n})}, \quad G^{-1} = \sum_{j=1}^n (s_j + a) \mathbb{1}_{(\frac{j-1}{n}, \frac{j}{n})}. \quad (21)$$

It follows quickly that $G^{-1} - F^{-1}$ is simply a constant function on $(0, 1)$ with value a , so the expression (19) simplifies to $|a|$. This concludes the second statement of the proposition.

Finally, let $S = \{0, 1, \dots, n-1\}$ and $T = \{1, 2, \dots, n\}$. As $T = S + 1$ is a translate of S , we have shown that $d_W^q(S, T) = 1 = d_H(S, T)$. However, $|T| = |S| = n$ while $|S \cap T| = n-1$, showing that no such inequality as (17) holds for the Wasserstein metric.

□

As a consequence of this translation property, the Wasserstein metric d_W^q may excessively grant an excessively high distance, and hence a low affinity, to two sets with a very high intersection. For example, if two sets of structural breaks are $A = \{100, 200, \dots, 900\}$ and $B = \{200, 300, \dots, 1000\}$, then d_{MJ}^p will reflect the high intersection and similarity between the sets A and B , while d_W^q will not. Indeed, for this example, $d_W^q(A, B) = 100$ while $d_{MJ}^p(A, B) = 100\left(\frac{1}{9}\right)^{\frac{1}{p}}$. That is, only the latter semi-metric assigns these remarkably similar sets of

structural breaks with a low distance, hence high affinity.

The Wasserstein metric would grant two time series that have quite similar structural breaks (and hence erratic behavior profiles) low affinity, and hence could include both in a portfolio. This would be a mistake, as such structural breaks as given by A and B in fact have almost all elements in common, and should be assigned high affinity, so the portfolio will not choose them both. We illustrate an example of this in Section 4.1.

4. Simulation study

In this section, we perform two experiments involving simulated time series with specified structural breaks. The first experiment illustrates the computation of the similarity between sets of structural breaks, comparing our MJ_p distance with the Hausdorff and Wasserstein metrics. The second experiment illustrates the allocation of assets in a sample optimization problem, together with constraints typical of an investment policy statement.

4.1. Synthetic Data simulation

First, we simulate a collection of time series x_1, \dots, x_n from a GARCH model (Lamoureux & Lastrapes, 1990) with m structural breaks determined by jumps at the points τ_1, \dots, τ_m . Each time series x_i follows a Student- t distribution with certain specified mean and variance functions. The mean function μ_t contains an autoregressive AR(1) process and a jump component; the latter is a product of a jump direction and magnitude with Bernoulli and gamma distributions, respectively. The variance function σ_t^2 contains several terms: an order one short term component, a long term persistence component, and a leverage effect component. We display four simulated simulated time series x_i with specified sets of structural breaks τ_j in Figure 1.

Figure 1 Four synthetic time series (a), (b), (c), (d) exhibiting dependence and correlation in jump behavior. The red annotated lines represent specified structural breaks.

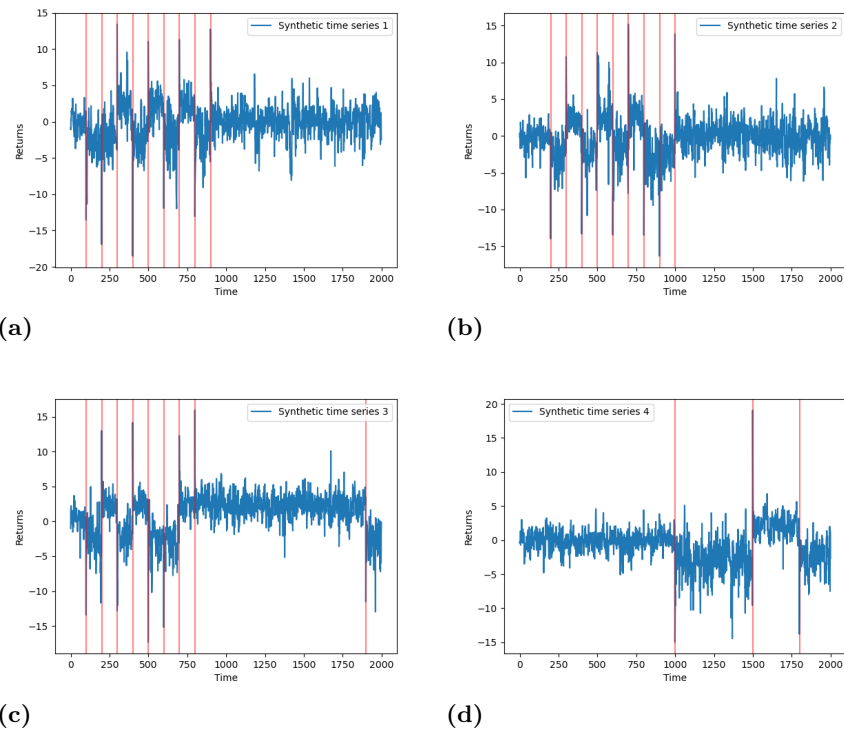


Table 1 Hausdorff distance matrix and affinity matrices between four synthetic time series' structural breaks.

$$D = \begin{bmatrix} 0 & 100 & 1000 & 900 \\ 100 & 0 & 900 & 800 \\ 1000 & 900 & 0 & 900 \\ 900 & 800 & 900 & 0 \end{bmatrix} A = \begin{bmatrix} 1 & 0.9 & 0 & 0.1 \\ 0.9 & 1 & 0.1 & 0.2 \\ 0 & 0.1 & 1 & 0.1 \\ 0.1 & 0.2 & 0.1 & 1 \end{bmatrix}$$

Table 2 Wasserstein distance matrix and affinity matrices between four synthetic time series' structural breaks.

$$D = \begin{bmatrix} 0 & 100 & 111 & 933 \\ 100 & 0 & 189 & 833 \\ 111 & 189 & 0 & 844 \\ 933 & 833 & 844 & 0 \end{bmatrix} A = \begin{bmatrix} 1 & 0.89 & 0.88 & 0 \\ 0.89 & 1 & 0.78 & 0.11 \\ 0.88 & 0.78 & 1 & 0.10 \\ 0 & 0.11 & 0.10 & 1 \end{bmatrix}$$

Table 3 $MJ_{0.5}$ distance matrix and affinity matrices between four synthetic time series' structural breaks.

$$D = \begin{bmatrix} 0 & 1 & 5 & 461 \\ 1 & 0 & 13 & 306 \\ 5 & 13 & 0 & 327 \\ 461 & 306 & 327 & 0 \end{bmatrix} A = \begin{bmatrix} 1 & 0.998 & 0.989 & 0 \\ 0.998 & 1 & 0.972 & 0.336 \\ 0.989 & 0.972 & 1 & 0.291 \\ 0 & 0.336 & 0.291 & 1 \end{bmatrix}$$

Table 4 MJ_1 distance matrix and affinity matrices between four synthetic time series' structural breaks.

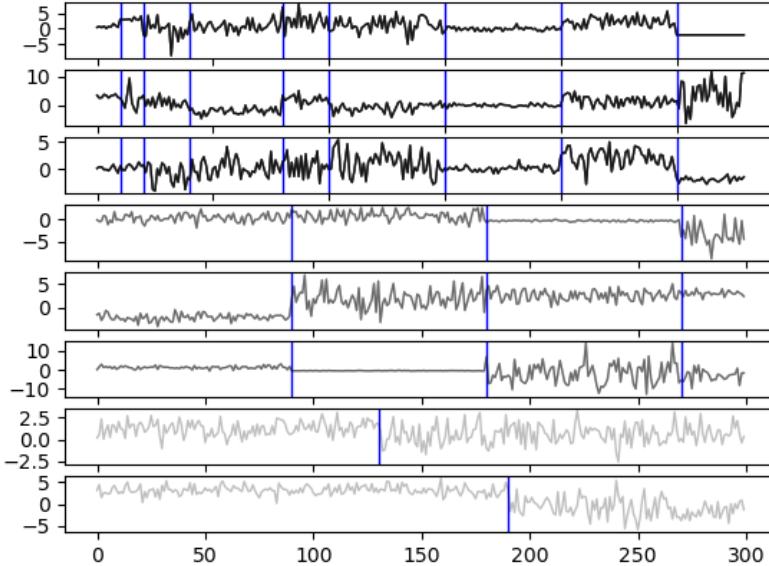
$$D = \begin{bmatrix} 0 & 11 & 61 & 517 \\ 11 & 0 & 72 & 417 \\ 61 & 72 & 0 & 367 \\ 517 & 417 & 367 & 0 \end{bmatrix} A = \begin{bmatrix} 1 & 0.98 & 0.88 & 0 \\ 0.98 & 1 & 0.86 & 0.19 \\ 0.88 & 0.86 & 1 & 0.29 \\ 0 & 0.19 & 0.29 & 1 \end{bmatrix}$$

Next, we compute the distance matrix and associated affinity matrix between the four synthetic time series, relative to the Hausdorff metric, Wasserstein metric, $\text{MJ}_{0.5}$ and MJ_1 semi-metric, respectively, and display them in Tables 1, 2 and 3, and 4. These tables collectively illustrate the advantages of the MJ_p semi-metrics compared to the Hausdorff and Wasserstein metrics first discussed in Section 3. First, the Wasserstein metric gives the lowest affinity score between the Time Series 1 and 2, which have 8 out of 9 of their structural breaks in common. These remarkably similar sets of structural breaks are given much lower distance and hence higher affinity under the $\text{MJ}_{0.5}$ and MJ_1 distances, illustrating Proposition 3.4. Next, the Hausdorff metric is far too sensitive to outliers; while TS1 and TS3 have 8 out of 9 points in common, these two time series are given the highest Hausdorff distance among the collection, hence affinity equal to 0. Similarly, TS2 and TS3 have 7 of 9 points in common, but their assigned affinity is 0.1. The Wasserstein, $\text{MJ}_{0.5}$ and MJ_1 distances all recognize the similarity between TS1 and TS3 (as well as TS2 and TS3), with high affinity scores. Once again the $\text{MJ}_{0.5}$ and MJ_1 perform better than the Wasserstein in discerning the strong similarity between these time series. We provide the time series TS4 as a reference time series that is quite distinct in its structural breaks from TS1, TS2 and TS3. Only the $\text{MJ}_{0.5}$ and MJ_1 assign TS1, TS2 and TS3 mutually high affinity scores, and only an algorithm using them to measure distances between sets of structural breaks would diversify away from including an unsuitably high quantity of TS1, TS2 and TS3 in one asset portfolio.

4.2. Synthetic data: portfolio optimization experiments

In this section, we apply our portfolio optimization methodology to synthetic data and illustrate the resulting allocation of assets. We generate 8 synthetic time series with specified structural breaks. For simplicity, Assets 1-3 have identical numbers of change points with identical locations, as do Assets 4-6; Assets 7 and 8 are outliers. In addition, we set all time series to have the exact same historical return $\mathbb{E}R_i$, so that the numerator of (7) is a positive constant,

Figure 2 Synthetic time series with fixed historical returns and specified structural breaks, identifying distributional changes. As the historical returns are kept constant, only the sets of structural breaks are used in the objective function (7).



regardless of the selection of weights. Thus, maximizing the MJ ratio (7) is equivalent to minimizing its denominator $\mathbf{w}^T \mathbf{A} \mathbf{w}$. We display the synthetic time series, together with structural breaks, in Figure 2. We allocate our portfolio subject to a typical constraint $5\% \leq w_i \leq 40\%, \forall i = 1, \dots, 8$.

Table 5 records the weights subject to the aforementioned constraints and conditions. The results demonstrate that our optimization framework is able to produce a more even distribution of change points across the portfolio. Assets 7 and 8, with significantly different breaks from the rest of the collection, are allocated more weight, 33.5% and 30.7%, respectively. Much less weight, 6.9%, is allocated to Assets 1, 2 and 3, and just 5% is allocated to Assets 4, 5 and 6. This experiment demonstrates that the algorithm provides diversification with regards to highly correlated structural breaks. Traditional mean variance

Table 5 Portfolio allocation results for synthetic data experiment in Section 4.2.

Asset	Number of change points	Weights
Asset ₁	8	6.9%
Asset ₂	8	6.9%
Asset ₃	8	6.9%
Asset ₄	3	5%
Asset ₅	3	5%
Asset ₆	3	5%
Asset ₇	1	33.49%
Assets ₈	1	30.7%

portfolio optimization would be unable to do so.

5. Real data results

In this section, we apply our methodology to real financial data. We envisage this method being suitable in an asset allocation context, so we use indices and commodities as our underlying candidate investments. We are essentially simulating the role of an asset allocator, such as a pension fund or endowment, interested in macroeconomic asset allocation decisions. There are 8 assets we allocate between to illustrate our method: the S&P 500, Dow Jones Index, Nikkei 225 Index, BOVESPA Index, Stoxx 50 Index, ASX 200, oil spot price, and gold spot price, all between January 2009 and November 2019. There are several important details and assumptions in our experiments on real data:

1. We train our algorithm over a relatively long period to estimate the true dynamics between various assets' structural breaks as precisely as possible. Training the algorithm on longer periods provides a more accurate assessment of similarity in varying market dynamics.
2. However, there is a balance between going back far enough to learn appropriate dynamics between asset classes and using too much history that relationships between assets no longer behave the way in which they were estimated. The behavior of individual asset classes and their relationships may change over time.

3. The period from January 2018 - June 2019 is a suitable out-of-sample period to test the algorithm, due to the varied market conditions. Most of 2018 provided relatively buoyant equity market returns, with a sharp drop in December 2018, followed by a prolonged recovery until June 2019. We wish to examine how candidate portfolios will perform in various market conditions, particularly in the presence of large drawdowns. In addition, we do not wish to test our algorithm during a period that is too similar to the training interval, as performance could be artificially strong. Thus, this is a suitable period to compare optimization algorithms' performance.
4. The role of asset allocation is often guided by an investment policy statement that provides upper and lower bounds for capital allocation decisions. This is captured in the candidate weights' constraints. During pronounced bull and bear markets, institutional asset allocators may not have the flexibility to implement global optimization solutions. For example, if two asset classes had significantly higher returns and lower volatility than the remainder of candidate investments, the unconstrained solution would allocate all portfolio weight into these two assets. Investment weighting constraints prevent these contrived scenarios from occurring. For our constraints, we place a minimum 5%, maximum 25% of portfolio assets in any candidate investment.
5. Our method provides an advantage over the simple correlation measure by addressing all three limitations in Section 2. One possible drawback to our proposed method, however, is that to learn meaningful relationships between assets' structural breaks, a long time series history is needed, preferably with many structural breaks observed.
6. When considering portfolio risk in an optimization framework, investors have a variety of measures they may choose to optimize over. Standard deviation, β , downside deviation and tracking error are just several of these. Our CPO model introduces a mathematical framework that addresses peak-to-trough (drawdown) losses and erratic behavior as a measure of risk.

Specifically, the model captures simultaneous asset shocks and aims to minimize the size of drawdowns by creating a uniform spread of change points across all portfolio holdings. We are unaware of any existing measure with these properties.

5.1. Training and validation procedure

We train the algorithm between January 2009 - December 2017 and test its performance on data from January 2018 - June 2019. The training procedure learns the weights allocated to each candidate investment using the aforementioned objective function and constraints. We compare our change point optimization method (CPO) with a more traditional mean-variance optimization (MVO) (Markowitz, 1952; Sharpe, 1966) under the same constraints.

First, we apply the Mann-Whitney change point detection algorithm to the training data (log returns between January 2009 - December 2017), identifying the locations of structural breaks in the mean for each possible asset. This yields 8 sets of change points, where each point is indexed by time. Following Section 2, we apply the $MJ_{0.5}$ semi-metric to determine the distance between candidate sets of breaks. We optimize the MJ ratio objective function in (7) with respect to the weights, determining candidate weight allocations. Finally, we run an out-of-sample forecasting procedure using the weights estimated in our training data. We compare the predictive performance of the CPO and MVO algorithms between January 2018 - June 2019. In addition, we apply hierarchical clustering to the resulting distance matrix between assets, as exploratory analysis of their similarity with respect to structural breaks. There are several interesting findings in our analysis:

1. Hierarchical clustering on the time series' structural breaks indicates that there is a cluster of four highly similar assets (S&P 500, Dow Jones, Stoxx 50, and oil), a cluster of three moderately similar assets (BOVESPA, Nikkei 225 and ASX 200) and an outlier in gold, displayed in Figure 3. These results confirm financial intuition and documented relationships between asset classes, in particular gold's properties as a safe-haven asset. Both the

S&P 500 and Dow Jones Index are determined to be in the same cluster, and accordingly quite similar. Given that there is significant overlap in the constituents of both indices, this is a logical finding.

2. The allocations of the CPO and MVO algorithms are quite different. In particular, the CPO algorithm allocates significantly more weight to gold and the ASX 200 Index, while allocating less weight to the S&P 500 Index, Stoxx 50, and oil, as seen in Table 6.
3. The MVO allocates 56.3% to the four indices in the highly similar cluster (S&P 500, Stoxx 50, Dow Jones and Oil). The CPO method allocates these indices a combined 21%. As expected, the change point optimization allocates less portfolio weight to assets with a high degree of similarity regarding their change points. Given that our aim with this new objective function is to smooth out returns, particularly during periods of extreme volatility such as market crises, the CPO does a superior job.
4. The CPO allocates 36% portfolio weight to gold, while the MVO allocates 17.6%. This higher allocation to gold is expected in this scenario, given the highly similar behavior and structural breaks of the other assets. It appears that the CPO method provides a more even distribution of weights across different types of financial assets.

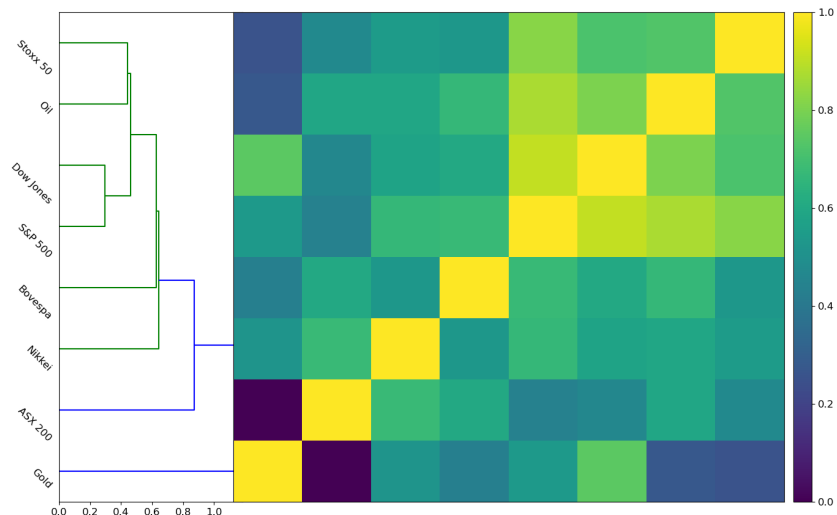
Table 6 Portfolio allocation results for real data according to the traditional mean-variance optimization (MVO) and our proposed change point optimization (CPO).

	S&P 500	Dow Jones	Nikkei 225	BOVESPA	Stoxx 50	ASX 200	Oil	Gold
MVO	0.16	0.05	0.05	0.05	0.18	0.1	0.17	0.17
CPO	0.05	0.05	0.05	0.075	0.225	0.25	0.05	0.25

5.2. Out-of-sample performance and distributional properties

After estimating the optimal allocation of weights for each asset, we compare the performance of the portfolio and properties of the predictive distribution

Figure 3 Hierarchical clustering applied to the distance matrix D_{ij} between eight real assets' structural breaks, as defined in Section 2. Results indicate the structural breaks are most similar among the Dow Jones, S&P 500, Stoxx 50 and oil. Gold is the most anomalous asset regarding structural break propagation.



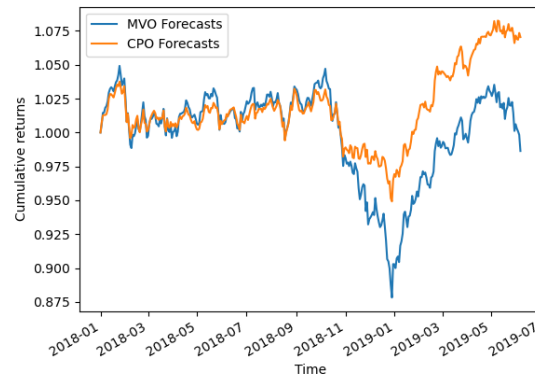
during the test period when using the MVO and CPO methods. Table 7 displays the final results when allocating the selected weights to each asset. We see immediately that the CPO method ended the period profitable by 7.0%, while the MVO method lost approximately 1.4% over January 2018 - June 2019. In addition, the CPO also produced a lower standard deviation, and a significant reduction in kurtosis (platykurtosis), relative to the MVO method.

We can see these features in more detail in Figure 4. First, Figure 4a shows the cumulative returns for each asset allocation strategy. The period during December 2018 displayed marked differences in performance. Although the MVO strategy was outperforming the CPO strategy until December 2018, the CPO strategy had a significantly smaller drawdown, as confirmed by Table 7. This is due to CPO's large position in gold, reducing the downward momentum of the total portfolio. Next, Figure 4b shows the two predictive densities, where the MVO density clearly exhibits fatter tails (leptokurtosis). That is, the CPO method provides consistently reduced volatility in returns. Overall, results demonstrate that the CPO algorithm provides a superior risk-adjusted return compared to the MVO with respect to a wide range of possible measures. Cumulative returns are greater, while volatility in returns is reduced. Most importantly, the size of the largest drawdown was reduced significantly.

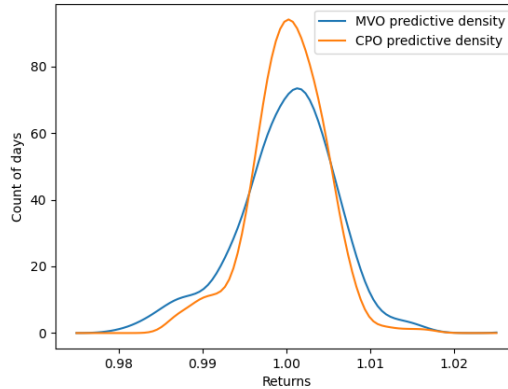
Table 7 Results of CPO and MVO methodologies applied to real data on the test period January 2018 - June 2019. CPO yields greater returns but less of all three risk measures: standard deviation, drawdown and kurtosis.

Optimization method	CPO	MVO
Cumulative returns	1.070	0.986
Mean	1.0002	0.99998
Standard deviation	0.0044	0.006
Drawdown	8.83	17.1
Kurtosis	1.06	1.55

Figure 4 Out-of-sample performance (a) and predictive densities (b) for the CPO and MVO methods during January 2018 - June 2019. Our methodology, CPO, generates superior returns and reduced drawdown, seen in (a), and reduction in kurtosis, seen in (b).



(a)



(b)

6. Conclusion

We have proposed a novel optimization method, which utilizes semi-metrics between sets of structural breaks, to reduce simultaneous asset shocks across an investment portfolio. Experiments on synthetic data confirm that we are able to detect similar time series in terms of structural breaks and accordingly allocate highly similar assets less portfolio weight. Experiments on real data suggest that our method may significantly reduce the size of portfolio drawdowns when compared to the traditional mean-variance framework. This novel optimization framework may have significant implications for asset allocation and portfolio management professionals who are interested in alternative measures of risk. Our method diversifies well away from portfolio drawdown, and seeks to avoid the erratic behavior of highly clustered change points. Our method is flexible, and different change point algorithms may be married with other distance measures or objective functions for alternative approaches.

There are several limitations in our optimization framework. Change point detection methodologies vary widely, and there is a substantial literature on their advantages and disadvantages (Hawkins & Zamba, 2005; Gustafsson, 2001). One potential limitation of our chosen change point detection algorithm is its deterministic selection (via hypothesis testing and maximization of test parameters) of change point locations. Alternative approaches, such as Bayesian methods, may provide a probabilistic approach incorporating the uncertainty around change points' existence. Next, our methodology requires a long training period to learn meaningful relationships between assets' structural breaks, and it is conceivable that such relationships from asset histories no longer hold in the present. Further, any distance measure between finite sets will have its limitations, such as the Hausdorff metric's sensitivity to outliers, semi-metrics' failure of the triangle inequality, or potentially excessive averaging in the MJ_p family.

Future research could work to ameliorate such limitations by building on the proposed framework. Different change point detection algorithms could be used

for other stochastic properties, such as the variance in the returns, or to reflect uncertainty in the breaks' existence. One could explore how results change when the order of p changes within the MJ_p semi-metric, or when entirely different distance measures are used between sets. More broadly, it is conceivable that one could diversify between sets through other means than reducing their discrepancy to a single scalar value. Further, one could combine our methodology, which requires a long history of training data, with alternative methods that give more weight to the recent behavior of a financial asset.

Appendix A. Change point detection algorithm

In this section, we describe the change point detection algorithm used in Section 2. The general change point detection framework is the following: a sequence of observations x_1, x_2, \dots, x_n are drawn from random variables X_1, X_2, \dots, X_n and undergo an unknown number of changes in distribution at points τ_1, \dots, τ_m . We assume observations are independent and identically distributed between change points, that is, between each change points a random sampling of the distribution is occurring. Ross (2015) notates this as follows:

$$X_i \sim \begin{cases} F_0 & \text{if } i \leq \tau_1 \\ F_1 & \text{if } \tau_1 < i \leq \tau_2 \\ F_2 & \text{if } \tau_2 < i \leq \tau_3, \\ \dots & \end{cases} \quad (\text{A.1})$$

While this requirement of independence may appear restrictive, dependence can generally be accounted by several means, such as modelling the underlying dynamics or drift process, then applying a change point algorithm to the model residuals or one-step-ahead prediction errors, as described by Gustafsson (2001). The change point models described below that we apply in this paper follow Ross (2015).

Appendix A.1. Batch detection (Phase I)

This first phase of change point detection is retrospective. We are given a finite sequence of observations x_1, \dots, x_n from random variables X_1, \dots, X_n . For simplicity, we assume at most one change point exists. If a change point exists at time k , this means observations have a distribution of F_0 prior to the change point, and a distribution of F_1 proceeding the change point, where $F_0 \neq F_1$. Then, one must test between the following two hypotheses for each k :

$$H_0 : X_i \sim F_0, i = 1, \dots, n \quad (\text{A.2})$$

$$H_1 : X_i \sim \begin{cases} F_0 & i = 1, 2, \dots, k \\ F_1, & i = k + 1, k + 2, \dots, n \end{cases} \quad (\text{A.3})$$

and select the most suitable k .

One proceeds with a two-sample hypothesis test, where the choice of test depends on the assumptions about the underlying distributions. Non-parametric tests can be chosen to avoid distributional assumptions. One appropriately chooses a two-sample test statistic $D_{k,n}$ and a threshold $h_{k,n}$. If $D_{k,n} > h_{k,n}$ then the null hypothesis is rejected and one provisionally assumes that a change point has occurred after x_k . These test statistics $D_{k,n}$ are normalized to have mean 0 and variance 1 and evaluated at all values $1 < k < n$; the largest value is assumed to be coincident with the existence of our sole change point. The test statistic is then

$$D_n = \max_{k=2, \dots, n-1} D_{k,n} = \max_{k=2, \dots, n-1} \left| \frac{\tilde{D}_{k,n} - \mu_{\tilde{D}_{k,n}}}{\sigma_{\tilde{D}_{k,n}}} \right| \quad (\text{A.4})$$

where $\tilde{D}_{k,n}$ are non-normalized statistics.

The null hypothesis of no change is rejected if $D_n > h_n$ for an appropriately chosen threshold h_n . In this case, we conclude that a (unique) change point has

occurred and its location is the value of k which maximises $D_{k,n}$. That is,

$$\hat{\tau} = \operatorname{argmax}_k D_{k,n}. \quad (\text{A.5})$$

This threshold h_n is chosen to bound the Type 1 error rate as is commonplace in statistical hypothesis testing. First, one specifies an acceptable level α for the proportion of false positives, that is, the probability of falsely declaring that a change has occurred when in fact it has not. Then, h_n is chosen as the upper α quantile of the distribution of D_n under the null hypothesis. For the details of computation of this distribution, one can see Ross (2015).

Appendix A.2. Sequential detection (Phase II)

In this second phase, the sequence $(x_t)_{t \geq 1}$ does not have a fixed length. New observations are continually received over time, and multiple change points may be present. Assuming no change point exists so far, this approach treats x_1, \dots, x_t as a fixed-length sequence and computes D_t as described in phase I. A change is flagged if $D_t > h_t$ for an appropriately chosen threshold. If no change is detected, the next observation x_{t+1} is brought into the sequence of consideration. If a change is detected, the process restarts from the data point immediately following the detected change point. Thus, the procedure consists of a repeated sequence of hypothesis tests.

In this sequential setting, h_t is selected so that the probability of incurring a Type 1 error is constant over time, so that under the null hypothesis of no change, the following holds:

$$P(D_1 > h_1) = \alpha, \quad (\text{A.6})$$

$$P(D_t > h_t | D_{t-1} \leq h_{t-1}, \dots, D_1 \leq h_1) = \alpha, \quad t > 1. \quad (\text{A.7})$$

In this case, assuming that no change occurs, the expected number of observations received before a false positive detection occurs is equal to $\frac{1}{\alpha}$. This quantity is often referred to as the average run length, or ARL_0 . Further details on appropriate values of h_t are detailed by Ross (2015).

References

Adams, R. P., & MacKay, D. J. C. (2007). Bayesian online changepoint detection. [arXiv:0710.3742](https://arxiv.org/abs/0710.3742).

Akoglu, L., Tong, H., & Koutra, D. (2014). Graph based anomaly detection and description: a survey. *Data Mining and Knowledge Discovery*, 29, 626–688. doi:10.1007/s10618-014-0365-y.

Almahdi, S., & Yang, S. Y. (2017). An adaptive portfolio trading system: A risk-return portfolio optimization using recurrent reinforcement learning with expected maximum drawdown. *Expert Systems with Applications*, 87, 267–279. doi:10.1016/j.eswa.2017.06.023.

Atallah, M. J. (1983). A linear time algorithm for the Hausdorff distance between convex polygons. *Information Processing Letters*, 17, 207–209. doi:10.1016/0020-0190(83)90042-x.

Atallah, M. J., Ribeiro, C. C., & Lifschitz, S. (1991). Computing some distance functions between polygons. *Pattern Recognition*, 24, 775–781. doi:10.1016/0031-3203(91)90045-7.

Baddeley, A. J. (1992). Errors in binary images and an L^p version of the Hausdorff metric. *Nieuw Arch. Wisk.*, 10, 157–183.

del Barrio, E., Giné, E., & Matrán, C. (1999). Central limit theorems for the Wasserstein distance between the empirical and the true distributions. *The Annals of Probability*, 27, 1009–1071. doi:10.1214/aop/1022677394.

Barry, D., & Hartigan, J. A. (1993). A Bayesian analysis for change point problems. *Journal of the American Statistical Association*, 88, 309–319. doi:10.2307/2290726.

Bhansali, V. (2007). Putting economics (back) into quantitative models. *The Journal of Portfolio Management*, 33, 63–76. doi:10.3905/jpm.2007.684755.

Brass, P. (2002). On the nonexistence of Hausdorff-like metrics for fuzzy sets. *Pattern Recognition Letters*, 23, 39–43. doi:10.1016/s0167-8655(01)00117-9.

Bridges, R. A., Collins, J. P., Ferragut, E. M., Laska, J. A., & Sullivan, B. D. (2015). Multi-level anomaly detection on time-varying graph data. In *Proceedings of the 2015 IEEE/ACM International Conference on Advances in Social Networks Analysis and Mining 2015* (pp. 579–583). ACM. doi:10.1145/2808797.2809406.

Calvo, C., Ivorra, C., & Liern, V. (2014). Fuzzy portfolio selection with non-financial goals: exploring the efficient frontier. *Annals of Operations Research*, 245, 31–46. doi:10.1007/s10479-014-1561-2.

Cappelli, C., Cerqueti, R., D’Urso, P., & Iorio, F. D. (2021). Multiple breaks detection in financial interval-valued time series. *Expert Systems with Applications*, 164, 113775. doi:10.1016/j.eswa.2020.113775.

Conci, A., & Kubrusly, C. (2017). Distances between sets - a survey. *Advances in Mathematical Sciences and Applications*, 26, 1–18.

Dubuisson, M.-P., & Jain, A. (1994). A modified Hausdorff distance for object matching. In *Proceedings of 12th International Conference on Pattern Recognition* (pp. 566–568). IEEE Comput. Soc. Press. doi:10.1109/icpr.1994.576361.

Eiter, T., & Mannila, H. (1997). Distance measures for point sets and their computation. *Acta Informatica*, 34, 109–133. doi:10.1007/s002360050075.

Fastrich, B., Paterlini, S., & Winker, P. (2014). Constructing optimal sparse portfolios using regularization methods. *Computational Management Science*, 12, 417–434. doi:10.1007/s10287-014-0227-5.

Fujita, O. (2013). Metrics based on average distance between sets. *Japan Journal of Industrial and Applied Mathematics*, 30, 1–19. doi:10.1007/s13160-012-0089-6.

Gardner, A., Kanno, J., Duncan, C. A., & Selmie, R. (2014). Measuring distance between unordered sets of different sizes. In *2014 IEEE Conference on Computer Vision and Pattern Recognition* (pp. 137–143). IEEE. doi:10.1109/cvpr.2014.25.

Gilchrist, W. (2000). *Statistical Modelling with Quantile Functions*. Chapman and Hall/CRC. doi:10.1201/9781420035919.

Gustafsson, F. (2001). *Adaptive Filtering and Change Detection*. John Wiley & Sons, Ltd. doi:10.1002/0470841613.

Hawkins, D. M. (1977). Testing a sequence of observations for a shift in location. *Journal of the American Statistical Association*, 72, 180–186. doi:10.1080/01621459.1977.10479935.

Hawkins, D. M., Qiu, P., & Kang, C. W. (2003). The changepoint model for statistical process control. *Journal of Quality Technology*, 35, 355–366. doi:10.1080/00224065.2003.11980233.

Hawkins, D. M., & Zamba, K. D. (2005). A change-point model for a shift in variance. *Journal of Quality Technology*, 37, 21–31. doi:10.1080/00224065.2005.11980297.

Iorio, C., Frasso, G., D'Ambrosio, A., & Siciliano, R. (2018). A P-spline based clustering approach for portfolio selection. *Expert Systems with Applications*, 95, 88–103. doi:10.1016/j.eswa.2017.11.031.

James, N., Menzies, M., Azizi, L., & Chan, J. (2020). Novel semi-metrics for multivariate change point analysis and anomaly detection. *Physica D: Nonlinear Phenomena*, 412, 132636. doi:10.1016/j.physd.2020.132636.

James, N., Menzies, M., & Chan, J. (2021). Changes to the extreme and erratic behaviour of cryptocurrencies during COVID-19. *Physica A: Statistical Mechanics and its Applications*, 565, 125581. doi:10.1016/j.physa.2020.125581.

Kocadağlı, O., & Keskin, R. (2015). A novel portfolio selection model based on fuzzy goal programming with different importance and priorities. *Expert Systems with Applications*, 42, 6898–6912. doi:10.1016/j.eswa.2015.04.047.

Koutra, D., Shah, N., Vogelstein, J. T., Gallagher, B., & Faloutsos, C. (2016). Delta-Con: Principled massive-graph similarity function with attribution. *ACM Transactions on Knowledge Discovery from Data*, 10, 1–43. doi:10.1145/2824443.

Lamoureux, C. G., & Lastrapes, W. D. (1990). Persistence in variance, structural change, and the GARCH model. *Journal of Business & Economic Statistics*, 8, 225–234. doi:10.2307/1391985.

León, D., Aragón, A., Sandoval, J., Hernández, G., Arévalo, A., & Niño, J. (2017). Clustering algorithms for risk-adjusted portfolio construction. *Procedia Computer Science*, 108, 1334–1343. doi:10.1016/j.procs.2017.05.185.

Li, J. (2015). Sparse and stable portfolio selection with parameter uncertainty. *Journal of Business & Economic Statistics*, 33, 381–392. doi:10.1080/07350015.2014.954708.

Magdon-Ismail, M., Atiya, A., Pratap, A., & Abu-Mostafa, Y. (). The maximum drawdown of the Brownian motion. In *2003 IEEE International Conference on Computational Intelligence for Financial Engineering, 2003. Proceedings*. (pp. 243–247). IEEE. doi:10.1109/cifer.2003.1196267.

Mansour, N., Cherif, M. S., & Abdelfattah, W. (2019). Multi-objective imprecise programming for financial portfolio selection with fuzzy returns. *Expert Systems with Applications*, 138, 112810. doi:10.1016/j.eswa.2019.07.027.

Markowitz, H. (1952). Portfolio selection. *The Journal of Finance*, 7, 77–91. doi:10.2307/2975974.

Moody, J., & Saffell, M. (2001). Learning to trade via direct reinforcement. *IEEE Transactions on Neural Networks*, 12, 875–889. doi:10.1109/72.935097.

Moreno, S., & Neville, J. (2013). Network hypothesis testing using mixed kronecker product graph models. In *2013 IEEE 13th International Conference on Data Mining* (pp. 1163–1168). IEEE. doi:10.1109/icdm.2013.165.

Peel, L., & Clauset, A. (2015). Detecting change points in the large-scale structure of evolving networks. In *Proceedings of the Twenty-Ninth AAAI Conference on Artificial Intelligence AAAI'15* (p. 2914–2920). AAAI Press.

Pun, C. S., & Wong, H. Y. (2019). A linear programming model for selection of sparse high-dimensional multiperiod portfolios. *European Journal of Operational Research*, 273, 754–771. doi:10.1016/j.ejor.2018.08.025.

Ranshous, S., Shen, S., Koutra, D., Harenberg, S., Faloutsos, C., & Samatova, N. F. (2015). Anomaly detection in dynamic networks: a survey. *Wiley Interdisciplinary Reviews: Computational Statistics*, 7, 223–247. doi:10.1002/wics.1347.

Rosenfeld, A. (1985). Distances between fuzzy sets. *Pattern Recognition Letters*, 3, 229–233. doi:10.1016/0167-8655(85)90002-9.

Ross, G. J. (2014). Sequential change detection in the presence of unknown parameters. *Statistics and Computing*, 24, 1017–1030. doi:10.1007/s11222-013-9417-1.

Ross, G. J. (2015). Parametric and nonparametric sequential change detection in R: the cpm package. *Journal of Statistical Software, Articles*, 66, 1–20. doi:10.18637/jss.v066.i03.

Ross, G. J., & Adams, N. M. (2012). Two nonparametric control charts for detecting arbitrary distribution changes. *Journal of Quality Technology*, 44, 102–116. doi:10.1080/00224065.2012.11917887.

Ross, G. J., Tasoulis, D. K., & Adams, N. M. (2013). Sequential monitoring of a Bernoulli sequence when the pre-change parameter is unknown. *Computational Statistics*, 28, 463–479. doi:10.1007/s00180-012-0311-7.

Sharpe, W. F. (1966). Mutual fund performance. *The Journal of Business*, 39, 119–138. doi:10.1086/294846.

Shonkwiler, R. (1989). An image algorithm for computing the Hausdorff distance efficiently in linear time. *Information Processing Letters*, 30, 87–89. doi:10.1016/0020-0190(89)90114-2.

Soleimani, H., Golmakani, H. R., & Salimi, M. H. (2009). Markowitz-based portfolio selection with minimum transaction lots, cardinality constraints and regarding sector capitalization using genetic algorithm. *Expert Systems with Applications*, 36, 5058–5063. doi:10.1016/j.eswa.2008.06.007.

Tanaka, H., Guo, P., & Türksen, I. (2000). Portfolio selection based on fuzzy probabilities and possibility distributions. *Fuzzy Sets and Systems*, 111, 387–397. doi:10.1016/s0165-0114(98)00041-4.

Vercher, E., Bermúdez, J. D., & Segura, J. V. (2007). Fuzzy portfolio optimization under downside risk measures. *Fuzzy Sets and Systems*, 158, 769–782. doi:10.1016/j.fss.2006.10.026.

Xuan, X., & Murphy, K. (2007). Modeling changing dependency structure in multivariate time series. In *Proceedings of the 24th international conference on Machine learning - ICML '07* (p. 1055–1062). ACM Press. doi:10.1145/1273496.1273629.